

Complementarity-based complementarity

Laura Serino,¹ Giovanni Chesi,² Benjamin Brecht,¹ Lorenzo Maccone,² Chiara Macchiavello,² and Christine Silberhorn¹

¹*Paderborn University, Integrated Quantum Optics, Institute for Photonic Quantum Systems (PhoQS), Warburgerstr. 100, 33098 Paderborn, Germany*

²*QUIT Group, Physics Department, Univ. Pavia, INFN Sez. Pavia, Via Bassi 6, 27100 Pavia, Italy*

(Dated: July 8, 2024)

We show that the amount of complementarity that a quantum system can exhibit depends on which complementary properties one is considering. Consider a set of mutually unbiased bases (MUBs) which corresponds to the spectral decomposition of some maximally complementary properties: The perfect knowledge of one, i.e. the state of the system is one of the basis states, implies that all the others are completely unknown, namely the measurement of another property will find any of its possible outcomes with uniform probability. We show that, depending on which three of the MUBs we choose, a 5-dimensional system can have different degrees of complementarity, measured using the minimum over all the system states of the sum of the entropies and of the variances of the measurement outcomes related to the three chosen observables. This property was first found experimentally, and demonstrates that an experimental discovery can disclose quantum information effects.

A property of a quantum system is described by an observable, namely a Hermitian operator \hat{O} . Each of the possible values o of the property \hat{O} is connected to an eigenstate $|o\rangle$. The Born-rule probability that the measurement of a system property has outcome equal to the value o is given by $|\langle o|\psi\rangle|^2$, where $|\psi\rangle$ is the system state. This state of affairs formalizes the principle of complementarity [1, 2]: A system can possess a definite value of a property, i.e. measurement outcomes have probability 1, only if its state is an eigenstate $|\psi\rangle = |o\rangle$ of that property. Otherwise, the value of that property is undefined, and only probabilistic predictions of measurement outcomes are possible. This implies that complementary properties exist: From a set of properties of the system, in general we can assign a definite (i.e. fully determined) value only to one.

In particular, maximally complementary properties exist: Assigning a definite value to one of them renders *all* the others maximally indeterminate, namely each of their outcomes will have uniform probability. This happens when we consider a set of observables whose eigenstates are mutually unbiased bases (MUBs). Indeed, the square modulus of the scalar product of any two states $|a_i\rangle, |b_j\rangle$ pertaining to two different MUBs is always $|\langle a_i|b_j\rangle|^2 = 1/d$, where d is the Hilbert space dimension.

Surprisingly, it was shown [3–5] that one can have large information on more than one complementary observable provided that the value of none of them is known with certainty (which would render the values of all the others completely indetermined). Namely, if the system is prepared in a state that is a nontrivial superposition when expressed in all the MUBs, then it is possible to have nontrivial *joint* information on multiple complementary properties.

Up to now a symmetry among different complementary properties (MUBs) was implicitly assumed. It was thought that a permutation of the MUBs would not change the information that one could have on them. In this paper we show that this belief is mistaken, by providing a counterexample in dimension $d = 5$ (where 6 MUBs exist). The information that a system can possess on three of the six complementary properties depends on *which* of the properties (MUBs)

are considered. We show this by calculating the lower bound of the sum of the entropies or of the variances of the measurement outcomes of three complementary observables, and prove that such a lower bound depends explicitly on the choice of complementary observables: Complementarity-based complementarity (Fig. 1). The analytic results are complemented by an experimental verification and by Monte-Carlo simulations where we calculate the sum of entropies and variances of random states.

The effect reported in this paper was first discovered experimentally while testing entropic uncertainty relations (EURs) in large dimensional Hilbert spaces.

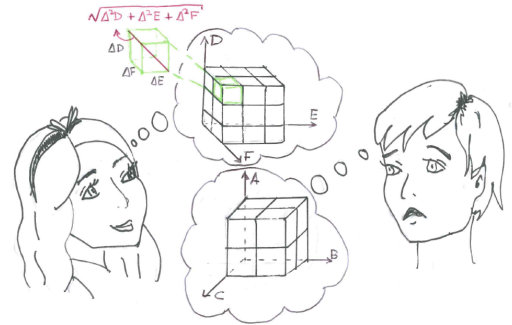


Figure 1. Alice and Bob are both interested in joint values of observables with mutually unbiased bases (MUB) as eigenstates. In dimension 5 there are 6 such observables: Bob measures observables A, B, C , Alice measures D, E, F . Surprisingly, Alice gets more information: she can divide the DEF phase space in smaller uncertainty blocks than Bob's, even though they are both looking at MUBs: the amount of complementarity among observables depend on which complementary observables, ABC or DEF , are considered.

Complementarity of three MUBs: Consider three maximally complementary observables $\hat{A}, \hat{B}, \hat{C}$ with mutually-unbiased eigenstates $|a_i\rangle, |b_j\rangle, |c_k\rangle$. One can have *partial* knowledge of all three of them if the state $|\psi\rangle$ is a non-trivial superposition when expressed in any of the bases $|a_i\rangle, |b_j\rangle, |c_k\rangle$. How much *joint* information on them can one

obtain? We need a quantification of how uncertain the outcomes of measurements of all three observables are. In the following, we concentrate on two quantifiers [6]. On the one hand, we consider the sum of the Shannon entropies $H(\hat{O}) = -\sum_j p_j \log_2 p_j$ of the Born probabilities $p_j = |\langle o_j | \psi \rangle|^2$ pertaining to the measurement of \hat{O} . The entropies are all positive quantities, so a small sum implies large *joint* knowledge. Moreover, the sum of entropies for maximally complementary observables has always a nontrivial lower bound given by the entropic uncertainty relations (EUR) [7–9]. On the other hand, we consider the sum of the variances [10] of $\hat{A}, \hat{B}, \hat{C}$. Differently from the entropy, the variance depends also on the eigenvalues of the observables, not only on the probabilities. We will choose observables with eigenvalues equal to a permutation $P(i)$ of the basis index i , i.e. $\hat{A} = \sum_i P(i) |a_i\rangle\langle a_i|$, and then minimize the variance $\Delta A^2 = \langle \hat{A}^2 \rangle - \langle \hat{A} \rangle^2$ over the permutations, to avoid effects due to the arbitrariness of the eigenvalue assignments. Also the sum of variances has a nonzero [11] lower bound for maximally complementary observables [12, 13].

We now show that the lower bound on the sum of entropies or variances of three different maximally complementary observables $\hat{A}, \hat{B}, \hat{C}$ depends on *the choice of the maximally complementary observables*, overturning an implicit belief that all MUBs are equivalent. This uncovers a hitherto unknown asymmetry in high dimensional systems.

We start from dimension $d = 5$ where there exist six maximally complementary observables $\hat{A}, \hat{B}, \hat{C}, \hat{D}, \hat{E}, \hat{F}$ with eigenvectors equal to the six MUBs [14, 15] $|a_i\rangle, |b_j\rangle, |c_k\rangle, |d_l\rangle, |e_m\rangle, |f_n\rangle$ presented in the appendix. In this case, we find that

$$H(\hat{A}) + H(\hat{B}) + H(\hat{C}) \geq 2 \log_2 5 \simeq 4.64386 \quad (1)$$

$$H(\hat{D}) + H(\hat{E}) + H(\hat{F}) \geq 4.43223\dots \quad (2)$$

The bound (1) was known [9] and was implicitly assumed to hold for every possible choice of MUB triplet, whereas the bound (2), obtained numerically (see in the appendix), was found while experimentally checking the entropic uncertainty relations. The states that minimize the first bound are eigenstates of any of the three $\hat{A}, \hat{B}, \hat{C}$, e.g. $|\psi\rangle = |a_0\rangle$. The states that minimize the second bound, instead, have a single null component when expressed in the computational basis $|a_i\rangle$, e.g. a state $\sum_n \psi_n e^{i\phi_n} |a_n\rangle$ with $\{\psi_n\} = (0.54488, 0.45067, 0, 0.45067, 0.54488)$, $\{\phi_n\} = (0, -2\pi/5, 0, \pi, -\pi/5)$. To validate the numerical minimization, we calculated the minimal sum of the entropies on a large number of states chosen randomly [16, 17] with Haar measure (Fig. 2), confirming that no state beats either bound (1), (2). We also checked that the sum of any *two* entropies never beats the Maassen-Uffink bound [8] of $\log_2 5$ (Fig. 3) and that the sum of *four* entropies has the unique lower bound found in Ref. [9] for every choice of the MUBs, confirming that the effect presented here requires exactly three MUBs.

We inspected all the $\binom{6}{3} = 20$ possible combinations of three MUBs out of 6 and found only the two bounds re-

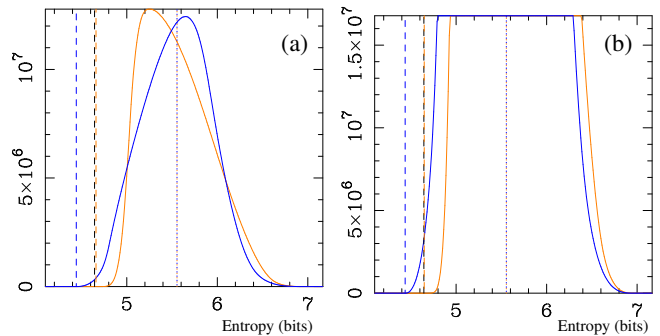


Figure 2. Monte-Carlo evaluation of the sums of entropies in (1) and (2) on states chosen randomly using the Haar measure. The histograms (250 bins) represent the number of states whose sum of entropies of three maximally complementary observables are equal to the value in the abscissa. (a) Simulation over 10^9 random states. (b) Detail of the tails of the distributions for a simulation over 10^{10} random states. The orange (blue) curves refer to the entropies of A, B, C (D, E, F). The black dashed line is at $2 \log_2 5$ and is approached by the left tail of the orange distribution, the blue dashed line approaches the lower bound of (2). The dotted lines are the (matching) average values of the two distributions at ~ 5.55 .

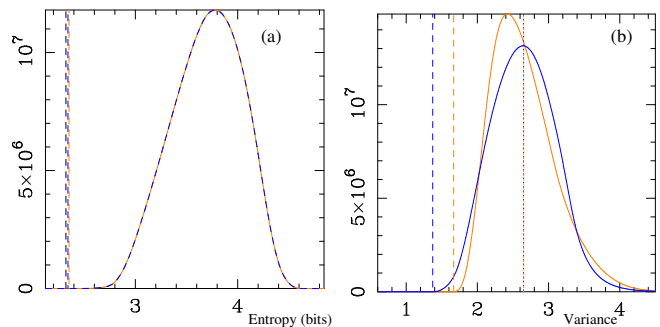


Figure 3. (a) Histograms of the Monte-Carlo evaluation of the sum of the entropies of two MUBs in dimension $d = 5$ (250 bins over 10^9 Haar distributed random states). As expected, all histograms match (here the histograms refer to A, B in orange and C, D in blue). The lower bounds of the left tails (orange-blue vertical dashed lines) approach the Maassen-Uffink bound $\log_2 5$ (black dashed line). (b) Histograms (250 bins over 10^9 states) of the sum of variances of three MUBs, evaluated over A, B, C (orange) with lower bound 1.67, and D, E, F (blue) with bound 1.37.

ported in (1), (2). Moreover, if a triplet could attain one bound, the remaining triplet would obtain the other bound. In particular, the triplets that only achieve the bound $2 \log_2 5$ are $ABC, ABF, BEF, ADE, BCD, CEF, CDF, BDE, ACE, ADF$; whereas the ones that achieve 4.43223.. are $ABD, ABE, ACF, BCE, DEF, CDE, BDF, ACD, BCF, AEF$.

Interestingly, even though it is known that there are two inequivalent classes of MUBs also in dimension $d = 4$ [14], we could not find a similar mismatch in the sum of entropies of three MUBs: for $d = 4$ there are 5 MUBs connected to five observables $(\hat{A}, \hat{B}, \hat{C}, \hat{D}, \hat{E})$, and we checked all $\binom{5}{3} = 10$

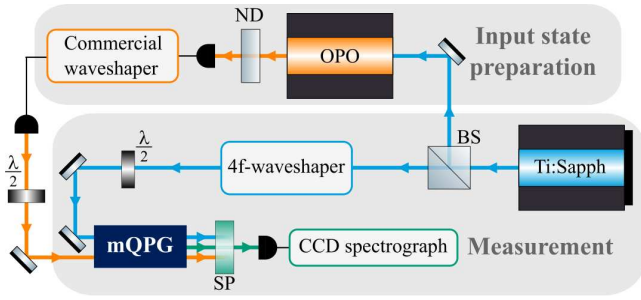


Figure 4. Schematic of the experimental setup. The signal (1545 nm) and pump (860 nm) pulses are generated by a Ti:Sapphire ultrafast laser with an optical parametric oscillator (OPO) at a repetition rate of 80 MHz. Two waveshapers generate the frequency-bin states in input from the signal pulse and the frequency-bin basis for the measurement from the pump pulse, respectively. In the mQPG waveguide, the signal modes are up-converted into a distinct output frequency based on their overlap with each pump mode. The output beam (552 nm) is separated from the unconverted signal and pump beams by a shortpass filter (SP) and then detected by a commercial CCD spectrograph (Andor Shamrock 500i).

combinations of triplets $\hat{X}, \hat{Y}, \hat{Z}$ in $\{\hat{A}, \hat{B}, \hat{C}, \hat{D}, \hat{E}\}$. They all have the lower bound $H(\hat{X}) + H(\hat{Y}) + H(\hat{Z}) \geq 3$ identified in Ref. [9]. However, while in the case $d = 3$ the states achieving the lower bound are the same for every triplet, in $d = 4$ the optimal states depend on the choice of the MUBs. We note that they share a common structure, i.e. they all have two non-null components.

By studying the sum of variances in $d = 4$ and $d = 5$ we find the same behavior of the uncertainty relation as the one found for the EURs: In $d = 4$ the optimal states attain the same minimum for every choice of the bases, while in $d = 5$ we find two distinct lower bounds dividing the triplets of MUBs in the same two sets as for the EURs. For $d = 4$ all the uncertainty relations for every choice of the three MUBs read

$$\Delta X^2 + \Delta Y^2 + \Delta Z^2 \geq 0.75 \quad (3)$$

with $\hat{X} \neq \hat{Y} \neq \hat{Z} \in \{\hat{A}, \hat{B}, \hat{C}, \hat{D}, \hat{E}\}$.

For $d = 5$, the uncertainty relation corresponding to the EUR in Eq. (1) reads

$$\Delta X^2 + \Delta Y^2 + \Delta Z^2 \gtrsim 1.67, \quad (4)$$

with XYZ in $\{ABC, ABF, BEF, ADE, BCD, CEF, CDF, BDE, ACE, ADF\}$; while the one related to the triplets in Eq. (2) is

$$\Delta D^2 + \Delta E^2 + \Delta F^2 \gtrsim 1.37, \quad (5)$$

which bounds also all the remaining triplets.

Experimental verification: We experimentally tested the entropic results presented in the previous section by encoding information in photonic time-frequency modes [18]. Namely, we consider a Hilbert space generated by broadband frequency bins and their superpositions encoded in coherent light

pulses. In this encoding alphabet, the five-dimensional computational basis $|a_i\rangle$ (associated to observable \hat{A}) is defined as a set of five Gaussian-shaped frequency bins centered at different frequencies, and the MUBs are generated by superimposing the fundamental bins with different phases. We note that the chosen alphabet falls in the category of pulsed temporal modes as the superposition states overlap in both time and frequency.

We perform the projective measurements using a so-called multi-output quantum pulse gate (mQPG) [19], a high-dimensional decoder for time-frequency pulsed modes based on sum-frequency generation in a dispersion-engineered waveguide. This device projects a high-dimensional input state onto all the eigenstates of a user-chosen MUB, selected via spectral shaping of the pump pulse driving the process, and yields the result of each projection in the corresponding output channel defined by a distinct output frequency.

Mathematically, we can describe the mQPG operation as a positive-operator-valued measure (POVM) $\{\pi^\gamma\}$, where each POVM element π^γ describes the measurement operator of a single channel set to detect mode γ [19–21]. Ideally $\pi^\gamma = |\gamma\rangle\langle\gamma|$; however, experimental imperfections lead to systematic errors in the POVMs, necessitating the more general description $\pi^\gamma = \sum_{ij} m_{ij}^\gamma |a_i\rangle\langle a_j|$, with $|a_i\rangle$ and $|a_j\rangle$ eigenstates of the computational basis. When measuring a pure input state $\rho^\xi = |\xi\rangle\langle\xi|$ from the chosen five-dimensional Hilbert space, we will obtain output γ with probability $p^{\gamma\xi} = \text{Tr}(\rho^\xi \pi^\gamma)$. In the measurement process, we use an mQPG with five channels, which can be programmed to perform projections onto any arbitrary MUB in the selected Hilbert space by assigning to each channel an eigenstate of that basis. Then, for each probed input state $|\xi\rangle$, we calculate the entropy in each measurement basis by estimating the probability p_i for each measurement outcome i as the normalized counts in the corresponding channel.

A schematic of the experimental setup is shown in Fig. 4. The signal and pump pulses, centered at 1545 nm and 860 nm respectively, are generated by a combination of a Ti:Sapphire ultrafast laser with an optical parametric oscillator (OPO) at a repetition rate of 80 MHz. The signal pulse is shaped by a commercial waveshaper to generate the frequency-bin states in input, whereas the pump pulse is shaped by an in-house-built 4f-waveshaper to generate the frequency-bin basis for the measurement. Both beams are coupled into the mQPG waveguide, where the signal modes are up-converted into a different output channel (corresponding to a distinct output frequency) based on their overlap with each pump mode, i.e., with each eigenstate of the chosen measurement basis. The output beam, centered at around 552 nm, is separated from the unconverted signal and pump beams by a shortpass filter and then detected by a commercial CCD spectrograph (Andor Shamrock 500i). The number of counts detected at each output frequency indicates the number of photons measured in the corresponding mode.

Results and discussion: For the experimental verification of the bounds (1) and (2), we probed different types of in-

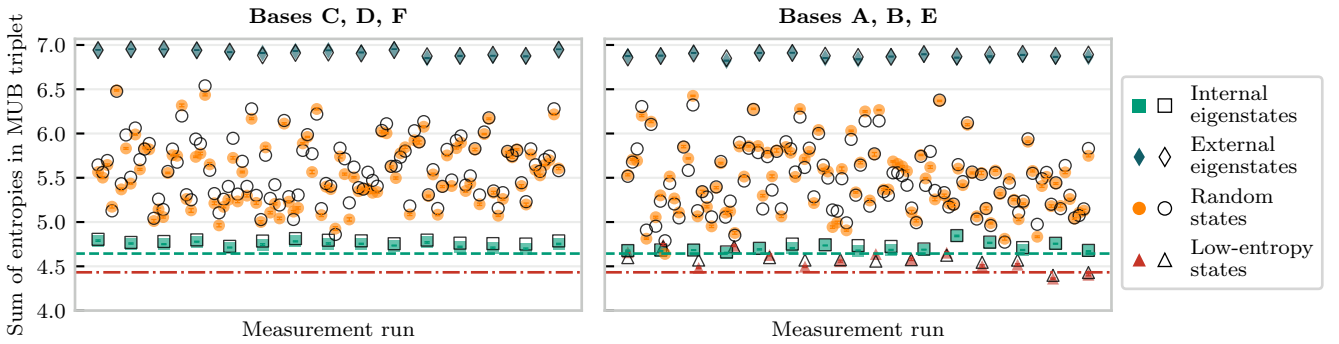


Figure 5. Sum of the entropies calculated in $d = 5$ for the two MUB triplets CDF (left) and ABE (right) for different types of input states: eigenstates of the MUBs in the selected triplet (green squares), eigenstates of the other MUBs (blue diamonds), random states (yellow circles), and low-entropy states that violate the previous assumption of bound (1) (red triangles). The filled markers show the experimental data, whereas the hollow markers describe the predicted results based on the characterized imperfect POVMs. The dashed green line and dash-dotted red line indicate the two lower bounds (1) and (2), respectively.

put states and, for each state, we calculated the entropy sum $H(\hat{X}) + H(\hat{Y}) + H(\hat{Z})$ from the measured output probabilities. The results for the two MUB triplets CDF and ABE are shown as filled markers in Figure 5, and compared to their respective lower entropy bounds (1) (green dashed line) and (2) (red dash-dotted line). For each input state, the error bars are calculated by sampling 500 sets of counts from a distribution with the measured mean and standard deviation of the original dataset and taking the 10%-90% spread of the corresponding entropy distribution. The error bars are not visible in most points due to their narrow extent.

The figure also shows the entropy values predicted via realistic simulations of the measurement process. These simulations are obtained by first characterizing the performance of the mQPG-based decoder through a quantum detector tomography [19, 22, 23] to reconstruct the actual POVMs. The average measurement error (cross-talk) per basis falls between 0.5% (for basis $|a_i\rangle$) and 1.9% (for basis $|f_n\rangle$). From the reconstructed POVMs, we calculated the expected entropy that one would observe measuring each state with this imperfect system, obtaining the hollow markers in Fig. 5. These estimates almost perfectly match the measured values, confirming that discrepancies with the theoretical predictions are to be attributed to the imperfect detection system.

The first type of probed input states are the eigenstates of all six MUBs, labelled “internal” if they are eigenstates of \hat{X} , \hat{Y} or \hat{Z} , and “external” otherwise. The entropy sum of the internal eigenstates (green squares) is always equal to the value predicted in (1) which, for the triplet CDF , is the minimum possible entropy sum. Contrarily, the external eigenstates (blue diamonds) always maximize the entropy sum.

Then we probed random input states (orange circles), generated by sampling amplitude and phase coefficients from a uniform distribution and renormalizing the amplitudes. We note that this method does not allow for truly uniform sampling of the parameter space; however, this is not relevant in the scope of this work, as we only look at random input states

to verify that they fall within the predicted entropy boundaries.

Finally, we probed states that are a superposition of four states of the computational basis $|a_i\rangle$, e.g. $\sum_n \psi_n e^{i\phi_n} |a_n\rangle$ with $\{\psi_n\} = (0.19323, 0.68019, 0, 0.68019, 0.19323)$ and $\{\phi_n\} = (-3\pi/5, \pi/5, 0, 0, 0)$ (red triangles in Fig. 5). These states were initially proven to minimize the sum of entropies in four, five and six MUBs in $d = 5$ [9]. However, while testing this assumption, we observed that the sum of entropies in the ABE triplet violated bound (1), previously assumed to hold for any possible choice of MUB triplet. This contradiction led to the discovery of bound (2) for the basis triplet ABE , while CDF maintains the known bound, revealing the underlying asymmetry between sets of MUBs.

Conclusions: In conclusion we have shown that the amount of joint information that one can have on maximally complementary observables can depend on which of them are considered, even though the overlap between the eigenstates of all maximally complementary observables are all the same, since they are MUBs. We showed that this holds in dimension $d = 5$ when the maximum joint information is gauged by minimizing the sum of the entropies and of the variances of three MUBs. For smaller dimensions, these metrics do not show this effect.

The authors acknowledge support from the EU H2020 QuantERA ERA-NET Cofund in Quantum Technologies project QuICHE. G.C. acknowledges support from from the PNRR MUR Project PE0000023-NQSTI. C.M. acknowledges support from the National Research Centre for HPC, Big Data and Quantum Computing, PNRR MUR Project CN0000013-ICSC, and from the PRIN MUR Project 2022SW3RPY. L.M. acknowledges support from the PRIN MUR Project 2022RATBS4 and from the U.S. Department of Energy, Office of Science, National Quantum Information Science Research Centers, Superconducting Quantum Materials and Systems Center (SQMS) under Contract No. DE-AC02-07CH11359.

Appendix

MUBs, explicit form: In the case $d = 5$, six MUBs are known. The explicit expression of the vectors for each basis is reported below as columns of the following matrices [14]:

$$\begin{aligned}
 \{|a_i\rangle\} &= \begin{pmatrix} 1 & 0 & 0 & 0 & 0 \\ 0 & 1 & 0 & 0 & 0 \\ 0 & 0 & 1 & 0 & 0 \\ 0 & 0 & 0 & 1 & 0 \\ 0 & 0 & 0 & 0 & 1 \end{pmatrix} \\
 \{|b_j\rangle\} &= \frac{1}{\sqrt{5}} \begin{pmatrix} 1 & 1 & 1 & 1 & 1 \\ 1 & \omega & \omega^2 & \omega^3 & \omega^4 \\ 1 & \omega^2 & \omega^4 & \omega & \omega^3 \\ 1 & \omega^3 & \omega & \omega^4 & \omega^2 \\ 1 & \omega^4 & \omega^3 & \omega^2 & \omega \end{pmatrix} \\
 \{|c_k\rangle\} &= \frac{1}{\sqrt{5}} \begin{pmatrix} 1 & 1 & 1 & 1 & 1 \\ \omega & \omega^2 & \omega^3 & \omega^4 & 1 \\ \omega^4 & \omega & \omega^3 & 1 & \omega^2 \\ \omega^4 & \omega^2 & 1 & \omega^3 & \omega \\ \omega & 1 & \omega^4 & \omega^3 & \omega^2 \end{pmatrix} \\
 \{|d_l\rangle\} &= \frac{1}{\sqrt{5}} \begin{pmatrix} 1 & 1 & 1 & 1 & 1 \\ \omega^3 & \omega^4 & 1 & \omega & \omega^2 \\ \omega^2 & \omega^4 & \omega & \omega^3 & 1 \\ \omega^2 & 1 & \omega^3 & \omega & \omega^4 \\ \omega^3 & \omega^2 & \omega & 1 & \omega^4 \end{pmatrix} \\
 \{|e_m\rangle\} &= \frac{1}{\sqrt{5}} \begin{pmatrix} 1 & 1 & 1 & 1 & 1 \\ \omega^2 & \omega^3 & \omega^4 & 1 & \omega \\ \omega^3 & 1 & \omega^2 & \omega^4 & \omega \\ \omega^3 & \omega & \omega^4 & \omega^2 & 1 \\ \omega^2 & \omega & 1 & \omega^4 & \omega^3 \end{pmatrix} \\
 \{|f_n\rangle\} &= \frac{1}{\sqrt{5}} \begin{pmatrix} 1 & 1 & 1 & 1 & 1 \\ \omega^4 & 1 & \omega & \omega^2 & \omega^3 \\ \omega & \omega^3 & 1 & \omega^2 & \omega^4 \\ \omega & \omega^4 & \omega^2 & 1 & \omega^3 \\ \omega^4 & \omega^3 & \omega^2 & \omega & 1 \end{pmatrix},
 \end{aligned}$$

where $\omega = e^{2i\pi/5}$.

In dimension four, we have five MUBs. Again, we display

them as columns of the following matrices [14],

$$\begin{aligned}
 \{|a_i\rangle\} &= \begin{pmatrix} 1 & 0 & 0 & 0 \\ 0 & 1 & 0 & 0 \\ 0 & 0 & 1 & 0 \\ 0 & 0 & 0 & 1 \end{pmatrix} \quad \{|b_j\rangle\} = \frac{1}{2} \begin{pmatrix} 1 & 1 & 1 & 1 \\ 1 & 1 & -1 & -1 \\ 1 & -1 & -1 & 1 \\ 1 & -1 & 1 & -1 \end{pmatrix} \\
 \{|c_k\rangle\} &= \frac{1}{2} \begin{pmatrix} 1 & 1 & 1 & 1 \\ 1 & 1 & -1 & -1 \\ -i & i & i & -i \\ i & -i & i & -i \end{pmatrix} \\
 \{|d_l\rangle\} &= \frac{1}{2} \begin{pmatrix} 1 & 1 & 1 & 1 \\ i & -i & i & -i \\ -1 & -1 & 1 & 1 \\ i & -i & -i & i \end{pmatrix} \\
 \{|e_m\rangle\} &= \frac{1}{2} \begin{pmatrix} 1 & 1 & 1 & 1 \\ i & -i & i & -i \\ i & -i & -i & i \\ -1 & -1 & 1 & 1 \end{pmatrix}.
 \end{aligned} \tag{7}$$

Numerical minimization: The numerical minimization we adopted here is very similar to the one exploited in Ref. [9]. We used the software package *Wolfram Mathematica*. We parametrized the states in dimension five as follows

$$\begin{aligned}
 |\psi\rangle &= \sin \alpha_1 \sin \alpha_2 \sin \alpha_3 \sin \alpha_4 e^{i\phi_1} |0\rangle + \\
 &\quad \cos \alpha_1 \sin \alpha_2 \sin \alpha_3 \sin \alpha_4 e^{i\phi_2} |1\rangle + \\
 &\quad \cos \alpha_2 \sin \alpha_3 \sin \alpha_4 e^{i\phi_3} |2\rangle + \cos \alpha_3 \sin \alpha_4 e^{i\phi_4} |3\rangle + \\
 &\quad \cos \alpha_4 e^{i\phi_5} |4\rangle,
 \end{aligned} \tag{8}$$

i.e. a parametrization yielding the normalization of the state intrinsically. Differently from Ref. [9], we checked the results of our optimizations by repeating the procedure twice: The first one, on re-parametrized states where the weights in Eq. (8) were permuted with respect to the states of the basis, and the second one on each of the re-parametrized states but expanded on the eigenstates of other MUBs. For each MUB $\{|x_k\rangle\}$ in Eq. (6) we retrieved the Born probabilities in terms of the coefficients in Eq. (8) through the superpositions between the states of the MUB and the generic state $|\psi\rangle$, namely

$$p(x_k) = |\langle x_k | \psi \rangle|^2. \tag{9}$$

Then we considered the Shannon entropies

$$H(\{|x_k\rangle\}) = - \sum_{k=1}^5 p(x_k) \log_2 p(x_k) \tag{10}$$

and the variances

$$\Delta X^2 = \langle \psi | \hat{X}^2 | \psi \rangle - \langle \psi | \hat{X} | \psi \rangle^2, \tag{11}$$

with $\hat{X} = \sum_k P(k) |x_k\rangle \langle x_k|$. We then minimized numerically the sum of three entropies and the sum of three variances for all possible triplets of distinct MUBs. In the case of the

variances, we also minimized over every permutation $P(k)$ of the eigenvalues k . The minimization was performed by using the routine NMinimize of *Wolfram Mathematica*, which finds the minimum of a function over a given set of parameters and constraints.

-
- [1] N. Bohr, *Naturwissenschaften* **16**, 245 (1928).
 [2] N. Bohr, *Nature* **121**, 580 (1928).
 [3] W. K. Wootters and W. H. Zurek, *Phys. Rev. D* **19**, 473 (1979).
 [4] D. M. Greenberger and A. Yasin, *Phys. Lett. A* **128**, 391 (1988).
 [5] B.-G. Englert, *Phys. Rev. Lett.* **77**, 2154 (1996).
 [6] We also considered the Renyi entropies of order 2 and 1/2, but the numerics gave inconclusive results.
 [7] D. Deutsch, *Phys. Rev. Lett.* **50**, 631 (1983).
 [8] H. Maassen and J. B. M. Uffink, *Phys. Rev. Lett.* **60**, 1103 (1988).
 [9] A. Riccardi, C. Macchiavello, and L. Maccone, *Phys. Rev. A* **95**, 032109 (2017).
 [10] D. A. Trifonov and S. G. Donev, *J. Phys. A: Math. Gen.* **31**, 8041 (1998).
 [11] Instead, the product of variances, as in the traditional Heisenberg-Robertson uncertainty relations [24], is problematic because it has no nonzero lower bound when minimizing over states: the product is null already if only one of the two variances is nonzero.
 [12] D. A. Trifonov, *J. Opt. Soc. Am. A* **17**, 2486 (2000).
 [13] D. A. Trifonov, *Eur. Phys. J. B* **29**, 349 (2002).
 [14] S. Brierley, S. Weigert, and I. Bengtsson, *Quantum Inf. Comput.* **10**, 0803 (2010).
 [15] T. Durt, B.-G. Englert, I. Bengtsson, and Życzkowski, *Int. J. Quantum Inf.* **8**, 535 (2010).
 [16] K. Życzkowski and M. Kuś, *J. Phys. A: Math. Gen.* **27**, 4235 (1994).
 [17] M. Poźniak, K. Życzkowski, and M. Kuś, *J. Phys. A: Math. Gen.* **31**, 1059 (1998).
 [18] B. Brecht, D. V. Reddy, C. Silberhorn, and M. G. Raymer, *Phys. Rev. X* **5**, 041017 (2015).
 [19] L. Serino, J. Gil-Lopez, M. Stefszky, R. Ricken, C. Eigner, B. Brecht, and C. Silberhorn, *PRX Quantum* **4**, 020306 (2023).
 [20] B. Brecht, A. Eckstein, R. Ricken, V. Quiring, H. Suche, L. Sansoni, and C. Silberhorn, *Phys. Rev. A* **90**, 030302(R) (2014).
 [21] V. Ansari, G. Harder, M. Allgaier, B. Brecht, and C. Silberhorn, *Physical Review A* **96** (2017), 10.1103/physreva.96.063817.
 [22] J. S. Lundeen, A. Feito, H. Coldenstrodt-Ronge, K. L. Pregnell, C. Silberhorn, T. C. Ralph, J. Eisert, M. B. Plenio, and I. A. Walmsley, *Nature Physics* **5**, 27 (2009).
 [23] V. Ansari, J. M. Donohue, M. Allgaier, L. Sansoni, B. Brecht, J. Roslund, N. Treps, G. Harder, and C. Silberhorn, *Phys. Rev. Lett.* **120**, 213601 (2018).
 [24] H. P. Robertson, *Phys. Rev.* **34**, 163 (1929).